

BRAIN COMMUNICATIONS

Lesion distribution and network mapping in dyskinetic cerebral palsy

 **Ana Luísa de Almeida Marcelino**,^{1,2,†}  **Bassam Al-Fatly**,^{1,†} **Mehmet S. Tuncer**,¹
Ingeborg Krägeloh-Mann,³  **Anne Koy**^{4,5} and  **Andrea A. Kühn**^{2,6,7,8,9}

† These authors contributed equally to this work.

Dyskinetic cerebral palsy encompasses a group of predominantly perinatally acquired complex motor disorders that present with dystonia and/or choreoathetosis and are frequently associated with brain lesions in neuroimaging. Recently, lesion network mapping provided a tool to redefine neurological disorders as circuitopathies. Elucidating the common networks impacted by lesions in this condition could pave the way to identify new targets for neuromodulatory therapeutic approaches. In this study, we aim to assess lesion distribution in dyskinetic cerebral palsy and identify a related functional network derived from lesions. Here, we review the literature of MRI findings in dyskinetic cerebral palsy and perform literature-based lesion network mapping. Articles reporting conventional MRI findings clearly attributable to affected patients were included for review. Imaging findings and their anatomical distribution were extracted and quantified according to an established MRI classification system for cerebral palsy. Reviewed articles were searched for figures depicting lesions and these were traced onto a paediatric template. Whole-brain functional connectivity from lesions causing dyskinetic cerebral palsy was calculated using a paediatric resting-state functional MRI connectome. Individual maps were thresholded and later overlapped to derive a common network map associated with dyskinetic cerebral palsy. Results were contrasted with two control datasets for spatial specificity. Review of 48 selected articles revealed that grey matter injury predominated (51%), followed by white matter injury (28%). In 16% of cases MRI was normal. Subcortical lesions affected the thalamus, pallidum and putamen in >40% of reported patients, respectively. Figures available from 23 literature cases were used to calculate the lesion network map of dyskinetic cerebral palsy. The lesion-derived map revealed functional connectivity to a wide network including the brainstem, cerebellum, basal ganglia, cingulate and sensorimotor cortices. The strongest connectivity was found for the motor thalamus. This study confirms subcortical grey matter lesions as the most common MRI finding in dyskinetic cerebral palsy. The neural network identified with lesion network mapping includes areas previously implicated in hyperkinetic disorders and highlights the motor thalamus as a common network node. These results should be validated and their therapeutic implications explored in prospective trials.

- 1 Movement Disorder and Neuromodulation Unit, Department of Neurology with Experimental Neurology, Charité - Universitätsmedizin Berlin, Corporate Member of Freie Universität Berlin and Humboldt-Universität zu Berlin, Berlin 10117, Germany
- 2 Berlin Institute of Health at Charité – Universitätsmedizin Berlin, 10117 Berlin, Germany
- 3 Department of Paediatric Neurology, University Children's Hospital Tübingen, 72076 Tübingen, Germany
- 4 Department of Pediatrics, Faculty of Medicine and University Hospital Cologne, University of Cologne, 50937 Cologne, Germany
- 5 Center for Rare Diseases, Faculty of Medicine and University Hospital Cologne, University of Cologne, 50937 Cologne, Germany
- 6 Bernstein Center for Computational Neuroscience, Humboldt Universität zu Berlin, 10117 Berlin, Germany
- 7 Exzellenzcluster NeuroCure, Charité - Universitätsmedizin Berlin, 10117 Berlin, Germany
- 8 Berlin School of Mind and Brain, Humboldt - Universität zu Berlin, 10117 Berlin, Germany
- 9 Deutsches Zentrum für Neurodegenerative Erkrankungen, 10117 Berlin, Germany

Received December 16, 2024. Revised May 14, 2025. Accepted June 11, 2025. Advance access publication June 13, 2025

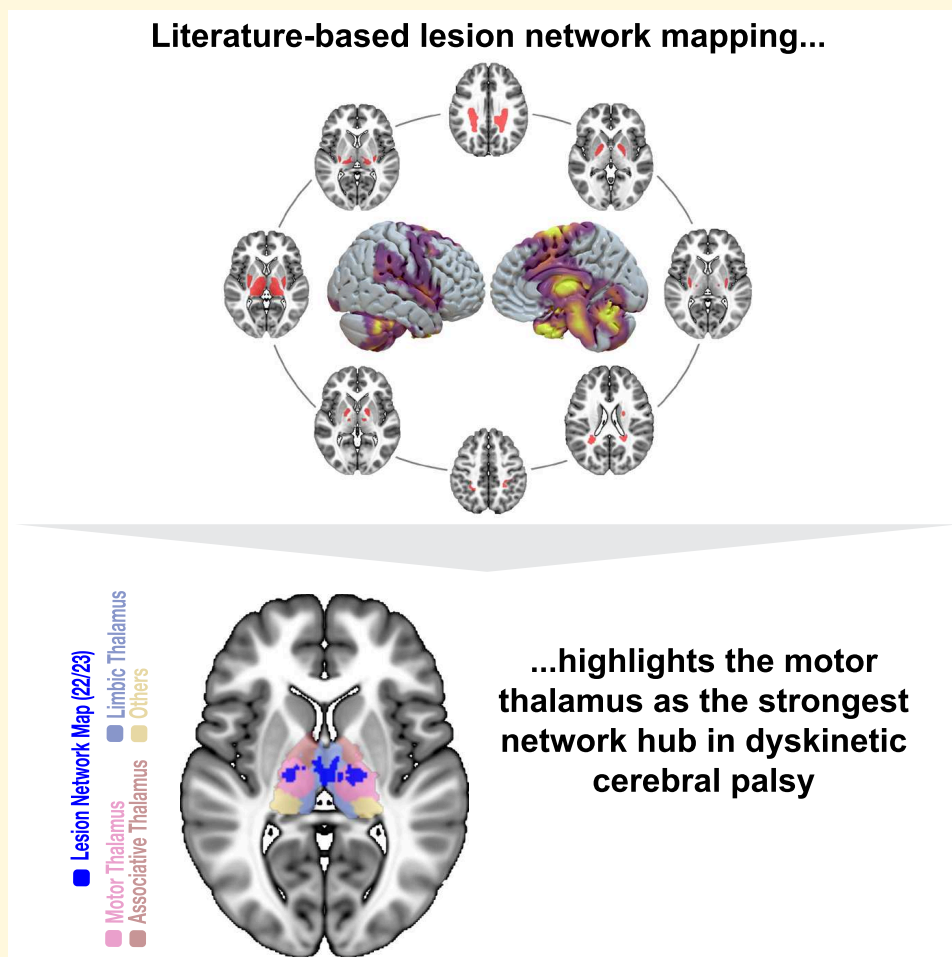
© The Author(s) 2025. Published by Oxford University Press on behalf of the Guarantors of Brain.

This is an Open Access article distributed under the terms of the Creative Commons Attribution License (<https://creativecommons.org/licenses/by/4.0/>), which permits unrestricted reuse, distribution, and reproduction in any medium, provided the original work is properly cited.

Correspondence to: Andrea A. Kühn
 Department of Neurology with Experimental Neurology at
 Charité – Universitätsmedizin
 Charitéplatz 1, 10117 Berlin, Germany
 E-mail: andrea.kuehn@charite.de

Keywords: dyskinetic cerebral palsy; neuroimaging; lesion pattern; lesion network mapping

Graphical Abstract



Introduction

Cerebral palsy (CP) is a descriptive term for disorders of movement and posture that result from a non-progressive injury or disturbance to the developing brain.¹ It can be classified into spastic, dyskinetic and ataxic according to the predominant neurological signs.² Dyskinetic cerebral palsy (DCP) represents at least 10–15% of all cases and is characterized by a complex movement disorder including dystonia and/or choreoathetosis.^{3–5} Although the diagnosis of DCP is

not based on aetiology, affected children often have a history of hypoxic ischemic encephalopathy or, more rarely, bilirubin encephalopathy. Additionally, stroke or cerebral infection can underlie the manifestations of DCP in term or preterm born infants.⁶ Currently available treatment options are solely symptomatic, and results are variable across patients. Thus, a deeper understanding of the common mechanisms underlying this complex and severely disabling hyperkinetic syndrome represents an urgent unmet clinical need.

Brain imaging shows predominantly grey matter injury including basal ganglia and thalamic lesions.^{4,7,8} However, the exact location within these regions and the frequency of lesions affecting distant areas such as the brainstem, the cerebellum or the hippocampus have not been investigated in detail. Emerging evidence suggests that specific neurological symptoms arise from network malfunction rather than as a consequence of localized brain pathology.^{9–11} For example, manifestation of cervical dystonia in adults has been linked to acquired lesions that were functionally connected to a network comprising the sensorimotor cortex and the cerebellum.¹⁰ Recently, further networks involved in movement disorders such as parkinsonism and hemichorea have been identified using lesion network mapping.^{12,13} This method assesses whole-brain connectivity from distributed lesions to investigate the network signature of specific neurological and psychiatric symptoms.⁹ In this line, the specific distribution of brain lesions associated with the occurrence of DCP could be harnessed to delineate the neural network that underlies DCP.

Lesion-derived networks were also demonstrated to explain clinical outcome after deep brain stimulation (DBS) in respective disorders like cervical dystonia¹⁰ or tics.¹⁴ In DCP, the clinical effects of pallidal DBS are variable but overall limited.^{15,16} Patients with more mobile movement components have been suggested to benefit more as compared to those that present with tonic dystonia.^{15,17} Understanding functional networks associated with DCP could pave the way to identify new targets for neuromodulatory therapeutic approaches.

In this study, we sought to assess current evidence on lesion distribution in DCP and use lesion network mapping of literature cases to derive a functional brain map representative of the DCP network. We considered relevant to provide the reader with a structured overview of the literature of imaging findings in DCP, as it brings our results into the context of current DCP research. Our literature review extends the results reported previously by Aravamuthan *et al.*⁷ by (i) including most recent studies (1990–2023), (ii) excluding any restrictions on aetiology of DCP and (iii) including only studies assessing imaging through MRI. For lesion network mapping, we used a paediatric resting-state fMRI connectome that has been recently implemented by our research group to enable functional network analyses in paediatric cohorts.¹⁸

Materials and methods

Systematic review

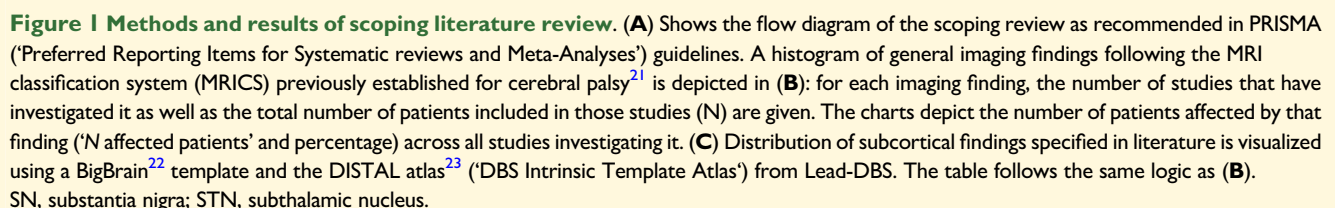
A systematic literature review was performed according to the guidelines of the Joanna Briggs Institute for scoping reviews.¹⁹ The pre-registered review protocol is available online on the Open Science Framework under <https://doi.org/10.17605/OSF.IO/N9F8B>. Reporting of the scoping review was guided by the adapted PRISMA guidelines ('Preferred Reporting Items for Systematic reviews and Meta-Analyses').²⁰ Results appear in shortened form in the manuscript (see Fig. 1) and can be found in detail in the supplementary files (Supplementary Tables 3 and 4).

A literature search was performed in October 2023 in Pubmed (search limits: 01.01.1990 and 05.10.2023) using 'cerebral palsy' and a descriptive term of the typically associated movement disorder such as 'dyskinetic', 'dystonia' or 'choreoathetosis' as well as 'neuroimaging' as search terms (details in [Supplementary methods](#), as in Aravamuthan *et al.*⁷). Full-text peer-reviewed articles written in English that contained MRI findings clearly attributed to this population were included, whereas studies that only included patients with normal MRI findings, where MRI was not performed, not sufficiently reported or not unequivocally attributable to the DCP population were excluded. Study types considered comprised observational, cohort and case-control studies as well as case series and individual case reports. Experimental/interventional study designs were included when baseline data was available. Reviews, comments, study protocols and editorials were excluded. Titles and abstracts of all studies were first screened and selected by one reviewer (A.L.d.A.M.). The full text of selected citations was reviewed once again for fulfilment of the inclusion criteria and reasons for exclusion were noted. A second reviewer (M.T.) screened the selected articles and, upon disagreement, discussed it with the first or a third reviewer (B.A.). References of the selected literature were screened for further suitable articles.

Evidence source data of the selected articles including study date, study type, study population, demographic data, classification system used for lesion description and main outcomes were extracted ([Supplementary Table 1](#)). Risk of bias was not specifically assessed. Imaging results, specifically the type of imaging findings and the anatomical localization of lesions, were extracted from the sources of evidence to a customized template adapted from the classification system MRICS,²¹ as this is the most widely implemented neuroimaging classification system for CP used in large registries.^{8,24} Thus, findings were assigned to the general categories 'white matter injury', 'grey matter injury', 'maldevelopments/malformations', 'miscellaneous/not specific' and 'normal'. As in MRICS, grey matter injury was further specified, when provided in this form, as 'BG/thalamus', 'cortico-subcortical lesions', 'focal ischemic/hemorrhagic infarctions'. Alternatively, the anatomical location of the subcortical injury was described, when given. Thus, if only the specific lesion location was named (e.g. thalamus and putamen), then it would only be reported in the 'specific subcortical findings' and not in the 'general findings' as grey matter injury. Studies that had one specific lesion pattern as inclusion criteria (e.g. pallidal lesions in Kernicterus in Kitai *et al.*²⁵) and have neglected other findings were excluded from the quantitative analysis of imaging findings to avoid reporting bias. Our reporting of the imaging findings included (i) number of studies assessing them, (ii) number of patients included in total in those studies and (iii) number (and percentage) of patients that have the imaging findings of interest.

Lesion network mapping

While assessing studies for eligibility, articles were screened for figures of MRI slices, which clearly illustrated lesions as



literature. Lesions were traced manually onto a paediatric MNI template using itk-SNAP (<http://www.itksnap.org>) and saved as binary masks.^{26,27} Of note, all lesions belonging to one literature-reported case were traced and saved in a single binary mask even if the lesions were in non-contiguous regions (e.g. putamen and thalamus) or in different slice levels. Functional connectivity seeding from these binary masks to

the rest of the brain was estimated for each lesion mask using the Lead-DBS (www.lead-dbs.org) tool Lead Mapper.²⁸

Briefly, blood-oxygen-level dependent (BOLD) signal was averaged in the seed region (the binary lesion mask) and correlated to the BOLD signal of each other voxel of the brain. Specifically, the functional connectivity was estimated using a paediatric functional connectome derived from resting-state fMRI of 100 neurotypical children²⁹ aged 6–18 years implemented in Lead-DBS (<https://www.lead-dbs.org/release/download.php?id=PedrsfMRI>).¹⁸ Voxel-wise R values were summarized across the connectome subjects using voxel-wise one-sample *t*-tests producing voxel-wise T-scores to represent lesion associated connectivity T-maps. Individual T-maps were thresholded at $T > 7$, binarized and later overlapped to identify a functional network (binary-overlap lesion network map-LNM) common to all lesions associated with the occurrence of DCP.¹⁴ The T-score thresholding corresponds to an uncorrected $P < 0.001$ and a family-wise error-corrected $P < 0.001$ in the current paediatric connectome.³⁰ In order to highlight maximally connected voxels to lesions, the produced LNM was arbitrarily thresholded to demonstrate voxels, which have connectivity to at least 95% of lesions. In order to investigate the robustness of the LNM, we calculated another LNM using FSL PALM (<https://fsl.fmrib.ox.ac.uk/fsl/fslwiki/PALM>). Briefly, a mass-univariate, one-sample *t*-test across the lesion T-maps was used to derive voxel-wise T-scores harnessing the randomized sign-flipping option in FSL PALM. This statistical analysis is based on permutation testing (5000×) and the voxel-wise resulting *P*-values were family-wise error (FWE) corrected for multiple comparison with an $\alpha < 0.05$.

Network specificity and stability analyses

We compared lesion connectivity profiles (T-maps) of DCP cases to those of two other cohorts. The aim of this comparison is to test the spatial specificity of the previously identified DCP-LNM. First, we used a cohort of focal cortical dysplasia (FCD) that leads to epilepsy in children.³¹ We refer to this cohort as ‘FCD’ cohort. The FCD lesions ($n = 78$) were already traced in native space and made available at (<https://openneuro.org/datasets/ds004199/versions/1.0.4>). We normalized the anatomical T1w MRI associated with each traced FCD lesion to the paediatric MNI template and applied the warp field to the corresponding tracing. We could only use 77 lesions as a final set in this cohort due to the presence of one lesion outside the brain mask. We then used the normalized tracing as a seed in the paediatric functional connectome and extracted the FCD-lesion associated connectivity profile as above (T-maps). In the second cohort, we created 100 lesion masks in the paediatric MNI template by generating spheres of 12 mm radius and masking them to include only grey matter voxel. We refer to this cohort as ‘Synth’ cohort. We then used the synthesized lesions as seeds in the functional connectome to derive the T-maps. We finally compared DCP-related T-maps to those of the other two cohorts using two-sample *t*-tests in FSL PALM

with 5000× permutations and voxel-wise correction for multiple comparison using FWE with an $\alpha < 0.05$.

Lastly, we sought to test the stability of the calculated network. For this purpose, we repeated LNM analysis by randomly leaving 5, 7 or 9 cases out of the calculation. One hundred different combinations of cases were first created in each of the leave-cases out option and the resulting LNM were spatially compared to the originally created LNM (including all cases) using spatial Pearson correlation.

Statistical analysis

Statistical tests used for lesion network mapping are described in detail in the sections above. Analyses were performed using Lead-DBS tools (www.lead-dbs.org) integrated in MATLAB software (The MathWorks Inc., Natick, MA, USA). *P*-values were corrected for multiple comparisons with family-wise error (FWE) when appropriate and considered statistically significant if $\alpha < 0.05$.

Results

Selected articles and study characteristics

General literature findings

From 535 articles that were initially screened, 91 papers were found eligible for further assessment (reasons for exclusion in Fig. 1A). After reading full text, 47 non-suitable articles were excluded and four articles were added manually, yielding a total of 48 articles included in the review. Individual study results and references are provided in the supplementary material (Supplementary Tables 3 and 4). Observational studies (23/48) made up the predominant study type and comprised national³² and international⁸ register studies. A total of 10147 patients were assessed in all studies, 1870 diagnosed with DCP. While 17/48 studies referred to SCPE (‘Surveillance of Cerebral Palsy in Europe’) guidelines as the standard definition of (D)CP, 27/48 studies did not specify the source of (D)CP definition used. Most studies included patients with hypoxic-ischemic encephalopathy, bilirubin encephalopathy or ‘other causes’ of DCP (36/48 studies). For 12 studies, the cause of DCP was not specified. The sex of included DCP patients was given for 34/48 studies and comprised 59.7% male. Age at inclusion of patients with DCP ranged from birth to 62 years (mean not calculated since different forms of reporting, available for 44/48 studies), birth weight and gestational age were more seldomly provided (16/48 and 18/48 studies, respectively). Further details regarding study outcomes are summarized in Supplementary Table 3.

Imaging findings

Age at MRI ranged from day 20 to 62 years (given for 24/48 studies) and reporting of neuroimaging results was standardized using an established classification system for CP such

as the MRICS,²¹ the preceding classification implemented by Krägeloh–Mann and colleagues³³ or as in Fiori *et al.*³⁴ in 16/48 studies. The first two classifications focus on lesion patterns and presumed timing of the insult, linking the findings to a stage of brain development. The classification by Fiori *et al.* focuses on neuroanatomical localization and quantification of imaging findings and aims to facilitate structure–function associations, as shown in Laporta-Hoyos *et al.*³⁵ for motor function, communication and cognition in DCP. Reporting of imaging findings was otherwise performed (individually) in extent as in clinical reports^{16,36–40} or guided by generalizable patterns of interest different from the abovementioned established classification systems.^{33,41–43} Neuroimaging findings were described to assess the prevalence of specific imaging patterns in CP population studies,^{4,8,44–47} to investigate imaging findings in specific aetiologies of DCP^{25,39,48–55} or associate them with clinical or functional outcomes.^{56–59} In other studies, imaging findings were included to supplement clinical or interventional findings (e.g. DBS, EEG)^{3,16,36,38,60–62} that were the primary focus of the study. Only six studies out of 48 investigated functional^{63,64} or structural^{41,42,65,66} connectivity measures in DCP.

Quantitative analysis and anatomical distribution of imaging findings

A total of eight studies were excluded from the quantitative analysis to avoid reporting bias (details [Supplementary Table 4](#)). Thus, data from 40 studies including imaging findings from 1181 DCP patients were available. First, general imaging findings of all DCP cases reported were summarized into the abovementioned categories according to the MRICS classification.²¹ In few cases, exceptions had to be made as two elements of different categories had been summarized together by the authors in the original paper (e.g. ‘cortical/subcortical’ lesions by Pr  el⁶⁷ include porencephaly, that could be considered a consequence of IVH and would otherwise be assigned to ‘white matter injury’). An overview of the general imaging findings is displayed in [Fig. 1B](#). Most common were grey matter injury found in 51% of reported patients (451/893 patients; 22 studies), followed by white matter injury 28% (281/1019; 24 studies), miscellaneous findings 13% (91/718; 15 studies), normal 16% (182/1140; 29 studies) and malformations 9% (74/786; 12 studies). Studies in which grey matter findings could be further specified revealed involvement of basal ganglia with/without thalamus in 50% (296/597; 18 studies), cortical/subcortical lesions 20% (116/571; 18 studies) and focal ischemic/hemorrhagic lesions 4% (8/195; 3 studies).

More than that, 25/40 articles discriminated subcortical findings ([Fig. 1C](#)): here, lesions were mostly found in the thalamus 51% (146/289; 18 studies), pallidum 45% (85/190; 14 studies) and putamen 43% (96/221; 15 studies). Structural abnormalities were also found in further remote areas such as the subthalamic nucleus, the corpus callosum, internal capsule, brainstem, substantia nigra, caudate

nucleus, cerebellum and hippocampus, however, more seldomly reported.

Network mapping of DCP-related lesions

Twenty-three cases of patients with DCP with a corresponding MRI figure were identified from 14 articles. The associated lesions are depicted onto a paediatric MNI template in [Fig. 2](#). Age at MRI ranged between 1 and 35 years. The lesions of these 23 cases were heterogeneously spatially distributed in the brain, with a tendency to affect the putamen, the thalamus or both in the majority of cases. Binary-overlap lesion network mapping revealed a functional brain network comprising the brainstem, cerebellum, thalamus, basal ganglia, cingulate and insular cortices as well as the sensorimotor cortex ([Fig. 3A](#)). This finding was replicated when using one-sample *t*-test method ([Fig. 3B](#)) and was stable when multiple iterations of different cases of lesions were used to recreate the network (see [Supplementary Fig. 3](#)). The lesion network map was also specific to DCP when compared with the FCD and the Synth cohorts ([Fig. 3C and D](#), respectively). Clusters of thalamic voxels demonstrated the strongest connectivity to lesion location in 95% of DCP cases ([Fig. 4](#)). The clusters correspond to the anatomical location of the mediodorsal nucleus and the ventral intermediate/ventral oral posterior nuclei (VIM/VOP; [Fig. 4C and D](#)). We sought to further segregate the functional part of the thalamus to which the lesions were maximally connected. As such, a *post-hoc* analysis exploring the connectivity strength of each lesion to the four functional thalamic parcellations (namely, motor, limbic, associative and other brain regions) was conducted (see [Supplementary Methods](#) and [Supplementary Fig. 1](#)). Since there is no paediatric functional parcellation of the human thalamus available, we built a thalamic parcellation atlas from the 100 subject normative paediatric connectome. A group comparison with ANOVA revealed a significant effect of functional connectivity to the different thalamic parcellations ($P < 0.001$). *Post-hoc* analyses via paired *t*-tests showed that functional connectivity to the sensorimotor parcellation of the thalamus was significantly higher than to associative and limbic parcellations ($P < 0.001$ in both cases; Bonferroni correction; see [Fig. 4B](#), right, for illustration and reported *P*-values). Since some of the cases present thalamic lesions, we controlled for redundancy by repeating the analysis ‘masking out’ the thalamic lesions as seeds. This control analysis revealed a similar thalamic cluster to that of the original analysis (see [Supplementary Fig. 2](#)).

Discussion

In this study, we performed a structured, comprehensive review of lesion distribution in DCP to delineate a lesion network map associated with this complex movement disorder. We show that while evidence of imaging findings in DCP comes predominantly from observational studies assessing the prevalence of general imaging patterns, specific

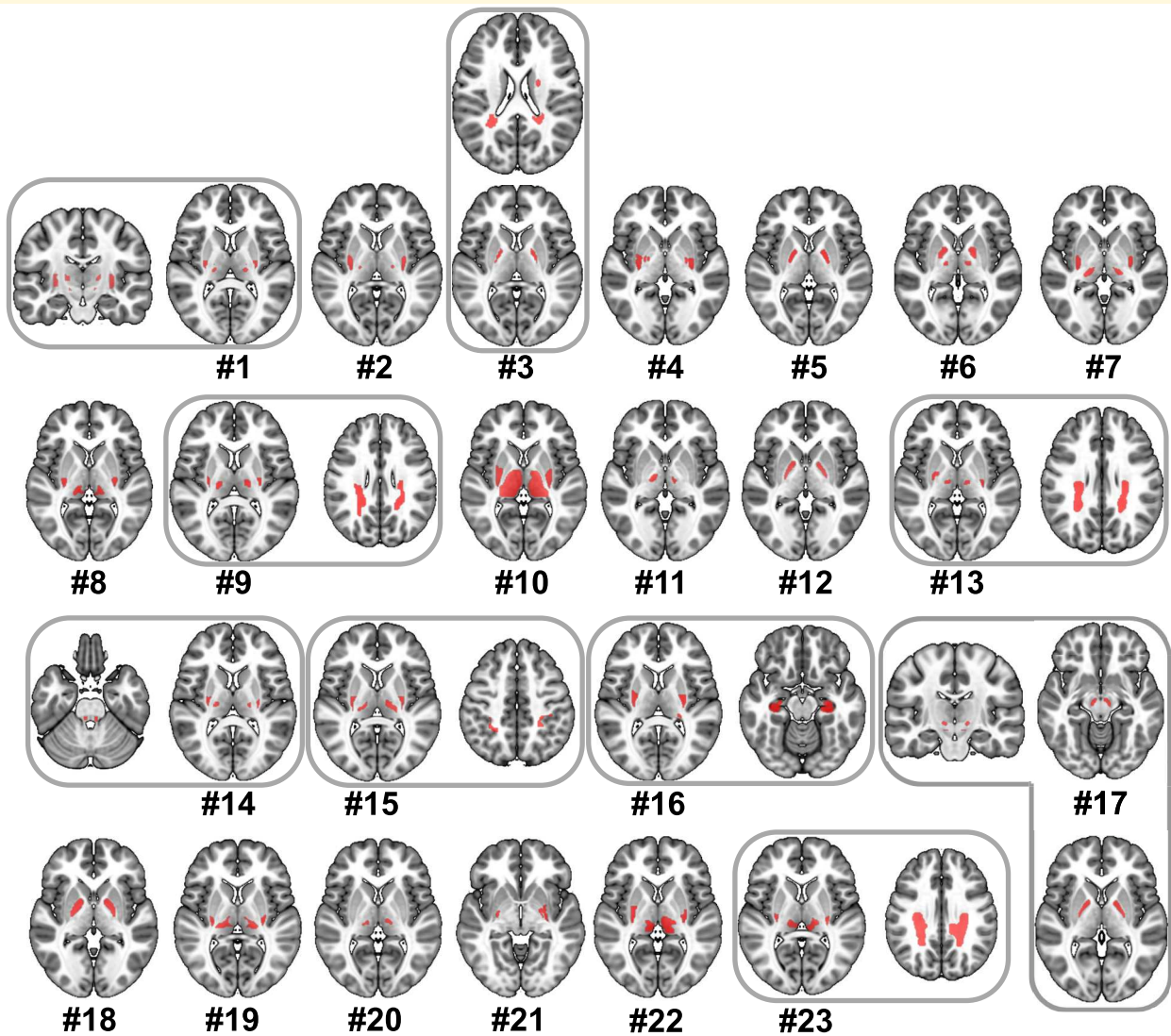


Figure 2 Spatial distribution of lesions associated with DCP. Each number represents an individual case from literature. Lesions were heterogeneously distributed in the putamen, globus pallidi, thalamus and white matter. Case #1 and #17 have additional subthalamic nucleus lesions, while case #14 has a brainstem lesion. It is noteworthy to mention that combined lesions occurring in single cases were taken as a single seed in the connectomic analysis.

lesion distribution is less frequently reported and includes remote subcortical areas. Our results of literature-based LNM reveal a distributed network including common motor network nodes such as the basal ganglia, cerebellum and sensorimotor cortex that have been previously implicated in hyperkinetic movement disorders. Importantly, the LNM reported here converges in the motor thalamus, which extends our current understanding of this disabling disease.

Clinicoanatomic insights from brain lesions in DCP

DCP is clinically defined by its presentation with hyperkinetic motor symptoms dominated by dystonia and choreoathetosis.^{1,5} The underlying aetiology is variable as well as the lesions that have been described in patients diagnosed

with DCP. Reviewing the literature, we show that most often the prevalence of specific imaging patterns is assessed in relation to CP subtypes^{8,45,69,70} (spastic or dyskinetic), different aetiologies²⁵ or gestational ages^{8,67} in observational (population-based) studies. Commonly used imaging classification systems underline the association between injury patterns and stages of cerebral development that has been proposed in the past.^{21,71} Our review results corroborate previous studies that reveal grey matter injury to be the most common imaging finding in DCP.⁸ An increased vulnerability of putaminal and thalamic neurons to hypoxia in the perinatal period as observed in HIE^{72,73} or of pallidal neurons to neurotoxic bilirubin as in BE⁷⁴ can explain frequent structural damage of these regions in DCP. Furthermore, individual differences in neuronal vulnerability or variability in the exposure to the damaging event

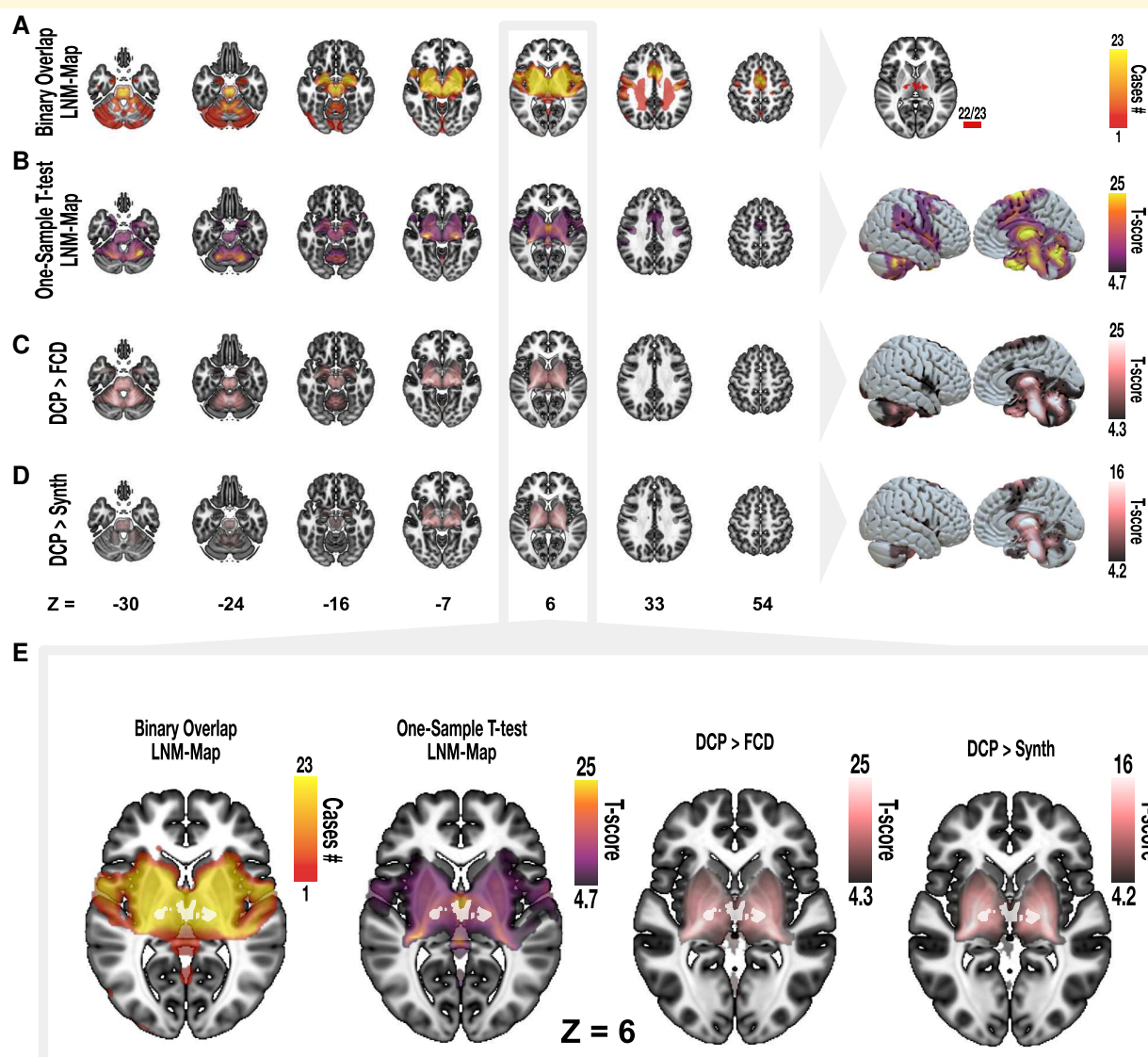


Figure 3 Lesion network mapping of DCP. Two mapping methods have been used to replicate the resulting lesion network map (LNM) for $N = 23$ DCP cases: a binary-overlap of T-maps thresholded to $T > 7$ is depicted in (A) which is later strictly thresholded to show only voxels of high connectivity to lesions. By running a permutation-based ($N = 5000$ permutations), one-sample t-test over all DCP-lesion T-maps, a network of significant voxels was determined which is statistically robust and thresholded to exclusively show voxels with family-wise error corrected $P < 0.05$ (B). To test for specificity of the resulting DCP-LNM, DCP-lesion associated connectivity profiles were compared to that of focal cortical dysplasia (C) and a synthesized set of lesions (D). Here, the areas highlighted in red were specific to DCP compared with the control cohorts. (E) Demonstrates the overlap of the highest connectivity cluster (white) on both DCP-derived maps (first two from left). Importantly, this same cluster was specific for DCP lesions when comparing with lesions in FCD or a synthetic cohort (two following slices). All voxel-wise t -scores (B–D) were corrected for multiple comparison using family-wise error using a P -value of < 0.05 . Backdrop of the volumetric slices is the skull-stripped T1w MRI modality of the paediatric MNI (4.5–18.5 years) template.²⁶ Surface rendering of the maps is depicted using a surface mesh of paediatric MNI template. FCD, focal cortical dysplasia; LNM, lesion network map.

may lead to different lesion patterns within the same DCP aetiology.^{75,76} In contrast to classical periventricular white matter injury that mostly disrupts the corticospinal tract and leads to spasticity, the basal ganglia are part of a more intricate circuit with complex local and remote connections, thus leading to more complex phenotypes.⁷⁷ For example, it is known that basal ganglia and thalamic injury patterns due to inherited (metabolic) diseases cause similar complex

dyskinetic phenotypes as seen in DCP.⁷⁸ Also, mutations in genes involved at different hubs of the basal-ganglia-thalamocortical loop can lead to complex dyskinetic movement disorders and mimic CP through cell-specific effects that do not necessarily reflect tangible lesion patterns in the MRI.⁷⁹

In this study, we focus on the common clinical presentation of DCP as a complex dyskinetic movement

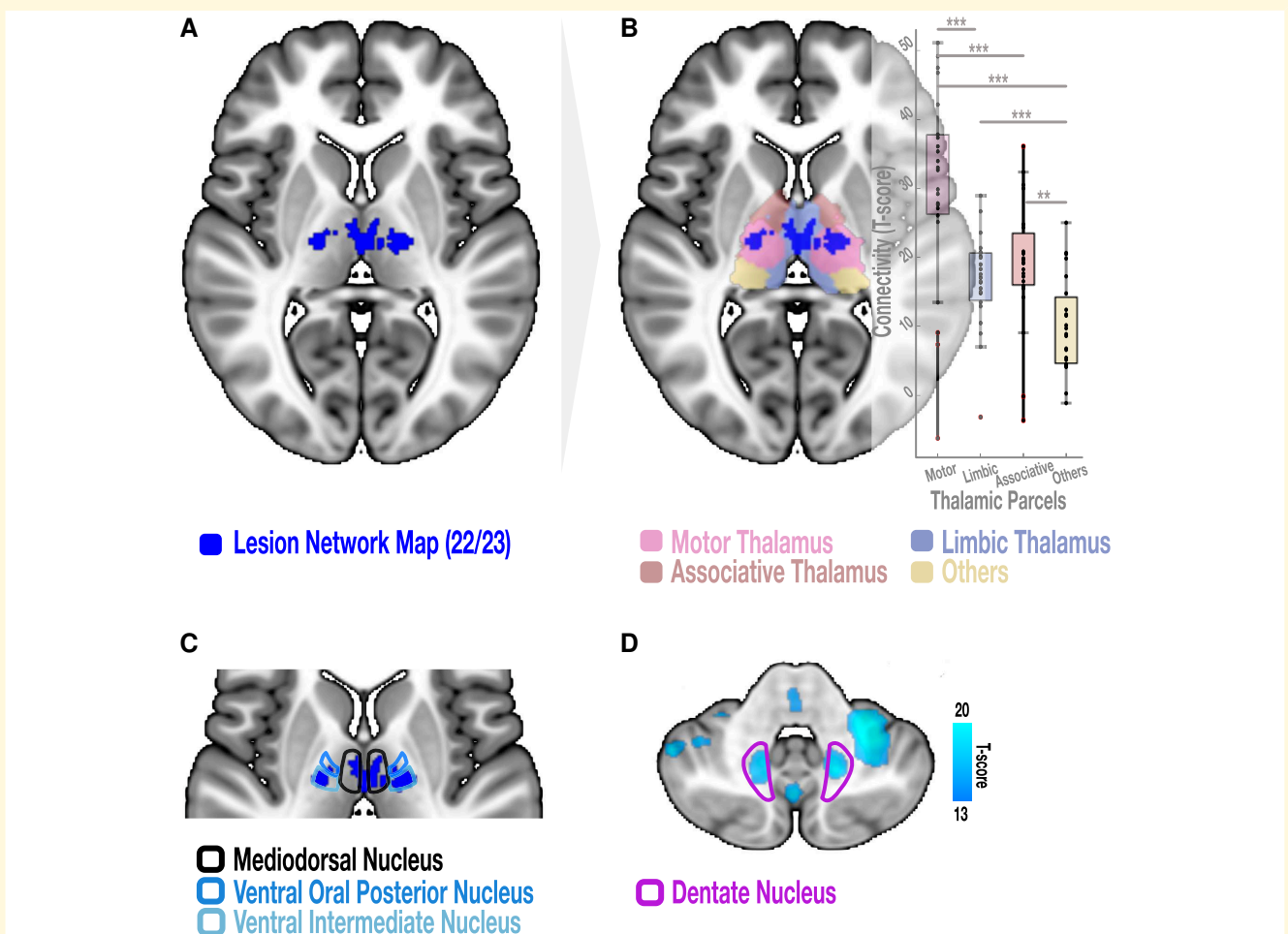


Figure 4 The thalamus as an important node of DCP-associated LNM. (A) Mapping lesions associated with DCP indicated a cluster of highest connectivity (connected to 22/23 cases) located in the thalamus (blue coloured cluster). This cluster was overlaid on a ‘winner-takes all’ functional thalamic parcellation (B) extracted using predefined cortical regions of interest (motor, associative, limbic and other cortical regions) in the 100 subjects of the paediatric resting-state fMRI connectome. Results are depicted as boxplots, where each individual datapoint represents the connectivity strength between a lesion and the respective thalamic parcellation of a single case. Connectivity to the motor thalamus was significantly higher than to any of the other thalamic parcels. The pairwise *t*-test *P*-values were reported as Family-wise error Bonferroni corrected *P*-values. The thalamic clusters highly connected to DCP lesions were located in the expected spatial location of the mediodorsal nucleus for the medial cluster and the ventral intermediate and ventral oral posterior nuclei for the lateral cluster (C). The lateral cluster agrees with a deep brain stimulation target previously used to treat paediatric dystonia including DCP.⁶⁸ The dentate nucleus, which has been recently targeted for deep brain stimulation in DCP⁶² is also overlapping with clusters identified in the one-sample *t*-test LNM (D). The latter LNM is highly thresholded to a T-score of (13/20) to better show the overlap. **P* < 0.05; ***P* < 0.01; ****P* < 0.001.

disorder and deliberately set no restrictions on its aetiology. Evidence regarding the association between specific motor phenotypes in DCP and imaging findings is scarce. While mixed-type DCP (dyskinesia and spasticity) has been associated with isolated or concomitant white matter injury, patients with isolated dystonia frequently present isolated basal ganglia lesions.⁵⁷ Monbaliu and colleagues³ observed a higher incidence of choreoathetosis in patients with ‘pure’ thalamus and basal ganglia lesions in comparison with mixed lesions (e.g. additional white matter lesions). However, specific movement disorder patterns or dyskinesia severity have not been systematically associated with specific imaging findings, for instance

using the dyskinesia impairment scale or kinematic analyses.

Our literature review shows that lesions leading to the clinical manifestation of DCP can be heterogeneously distributed within the basal ganglia nuclei or thalamus but can also affect remote locations such as the corpus callosum, internal capsule, brainstem, hippocampus or cerebellum. Within the framework of movement disorders being considered network disorders, we postulate that despite different putative lesion mechanisms and lesion distribution they have in common the perturbation of a DCP-specific functional network. We set out to apply lesion network mapping to our literature findings to explore this hypothesis.

Towards a network signature of DCP

Recent advances in brain mapping and connectomic analyses have contributed to redefine neurological diseases as network disorders. Lesion network mapping (LNM) is exemplifying this paradigm shift in the approach to neurological diseases and has allowed to identify relevant brain networks in different conditions including movement disorders.^{10,11,14} The current study is a further use case of LNM in a paediatric neurological disorder. Our results partially corroborate previous findings of LNM in chorea and dystonia in adult populations.^{10,13} Regions like the cerebellum, anterior cingulate cortex, thalamus, globus pallidus, putamen and the brainstem were indeed parts of the LNM in chorea and dystonia. Although the motor cortex was negatively correlated in terms of connectivity to lesions causing dystonia, it was positively connected to lesions causing chorea in adults.^{10,13} Noteworthy, even though terminology of childhood movement disorders is derived from adults, specific features in clinical presentation differ and underlying mechanisms cannot be transferred one-to-one.⁵ The aforementioned regions comprise important hubs in motor control previously associated with complex hyperkinetic syndromes of different aetiologies in childhood.⁷⁹ Perturbation of such networks during a critical timepoint in brain development adds complexity to the symptoms encountered in children as compared to focal lesions to the adult brain.^{80,81} The use of a paediatric connectome in our study aimed to account for this relevant aspect in paediatric disorders.

Previous studies have demonstrated evidence of structural or functional changes in DCP patients in different regions of the LNM demonstrated here. Qin and colleagues found reduced interhemispheric connectivity in motor network areas including the cerebellum, motor cortex, supplementary motor area and anterior cingulate cortex⁶⁴ as well as altered functional connectivity within cerebellar, sensorimotor and left frontoparietal resting state networks⁶³ in patients with DCP. Structural connectivity studies indicated reduced white matter integrity in motor tracts including the corticospinal tract as well as cerebellar connections and association fibres related to speech and language.^{41,42} On a structural network level, reduction of white matter connectivity measures was associated with impaired motor and cognitive skills.⁶⁶ Altered functional and structural connectivity measures found in these studies indicate a more widespread impact of brain lesions on neural networks that are not always captured by conventional MRI measures. Importantly, the network identified in our analysis included areas previously known to show hypometabolism in DCP caused by hypoxic ischemic encephalopathy and Kernicterus; namely, the cerebellum, the brainstem, the putamen and the thalamus (Supplementary Fig. 4 depicts significant peak regions).^{82,83} This convergent evidence reinforces the importance of the pathophysiological contribution of these regions to DCP and indicates involvement of a widespread neural network beyond the structurally damaged areas. This finding is also relevant to cases of DCP without imaging abnormalities (as

in 16% of cases identified in our review process), for which one could speculate on a subtle metabolic lesion or dysfunction on a cell-specific level that affects the here deciphered LNM even if no structural damage is detectable on imaging.

The finding that almost all DCP lesions included in the current study are strongly connected to the motor thalamus highlights the central role of this particular hub of the motor network. In fact, thalamic stroke has been previously shown to cause complex hyperkinetic movement disorders.⁸⁴ The thalamus integrates information from the basal ganglia, the cerebellum and sensory afferents in complex circuitries to inform cortical dynamics.⁸⁵ Even though traditionally assigned to the basal ganglia, encoding of action selection and movement vigor in the motor thalamus has been shown to influence movement kinematics in rodents.⁸⁶ Also, the temporal dynamics of thalamo-cortical interactions are crucial for intact motor execution.⁸⁷ Thus, altered spatio-temporal precision of signal processing throughout the identified network may be one possible explanation for manifestation of complex hyperkinetic movement disorders after lesions structurally or functionally affecting the motor thalamus. Specifically, investigation of thalamocortical connectivity in patients with perinatal lesions in relation to motor outcome could further elucidate these mechanisms. Lastly, highest connectivity of lesions identified in the current study to the thalamic cluster mimic previous LNM findings of strongest connectivity from lesions to subcortical structures in different movement disorders.^{10,11,13,14} This suggests a pivotal role of these subcortical nodes (namely basal-ganglia and thalamus) in orchestrating the pathological impact of lesions.

Implications for future studies

We propose that the evidence provided in this literature-based study can motivate generation of new hypotheses for future diagnostic and treatment studies of DCP. For example, studies following our approach in a larger cohort could elucidate the impact of specific lesion patterns on brain networks to eventually predict patients at risk and symptom severity in CP. In addition, applying connectomics to clinically well-characterized DCP cohorts could allow disentangling different motor phenotypes and respective imaging findings. This, along with knowledge regarding treatment responses may help to better understand the underlying pathophysiology of DCP and allow identification of new targets for neuromodulatory interventions such as DBS. Currently, the globus pallidus pars internus is commonly targeted for DBS in childhood dystonia of different aetiologies, including DCP.⁸⁸ However, due to variable clinical effects^{15,16} and anatomical complexity associated with the presence of lesions, alternative targets such as the VIM/VOP thalamic nuclei⁶⁸ and recently the dentate nucleus⁶² have been suggested. Intriguingly, all these DBS targets lie within the DCP-lesion network identified in our study (Fig. 4C and D depicts the relationship of DCP-LNM to alternative DBS targets). Of note, DCP causative lesions demonstrated the highest connectivity to the VIM/VOP target. Even though the pallidum and the dentate display

different connectivity strengths, they reside within the identified DCP network. The association of lesion-derived and therapeutic networks has been demonstrated for tics and dystonia in adults with Tourette syndrome¹⁴ and isolated idiopathic dystonia,¹⁰ respectively. In DCP, the implanted DBS system should counteract the dysfunctional network effect of lesions. Lastly, the motor cortex is another hub of the LNM identified here, which could serve as a target for non-invasive stimulation techniques. In one study, cathodal transcranial direct current stimulation over the motor cortex was probed to downregulate excessive activity found in this area with variable success in controlling motor symptoms in a small sample size.⁸⁹ Assessing the impact of such therapeutic options would require further prospective clinical trials.

Limitations

Literature-based studies are limited by the fact that they attempt to summarize a heterogeneous body of evidence that has emerged due to different questions and using different approaches. Reporting of imaging findings was standardized using previously established classification systems in >30% of studies included, yielding higher comparability between studies. However, focusing on predominating lesion patterns leads to a reporting bias, thus possibly neglecting important structural findings.^{21,34} The use of a standardized definition of (D)CP has not been stated in all studies, which could affect generalizability of results. In addition, lesion location at a 'macro' scale only explains part of variance in clinical manifestation. Hypoxic ischemic encephalopathy, but also genetic syndromes that cause specific lesion patterns (e.g. PDE10A mutations) and can be included in DCP cohorts, present a specific neuronal vulnerability that will not be sufficiently reflected in imaging patterns. Of note, current literature indicates a high prevalence (>50%) of concomitant dystonia in predominant spastic CP with isolated periventricular leukomalacia in MRI that was not accounted for in this study design as we focused on DCP as the common clinical phenotype.⁹⁰ Also, concurrent epilepsy could not be controlled for in literature cases when comparing with FCD lesions due to lack of systematic reporting of comorbidities in reviewed cases. Another limitation of performing LNM from literature is that imaging slices are rendered in 2D. However, it has been demonstrated that seeding from 2D lesions in functional connectomes is similar to 3D volumetric lesions.⁹¹ The small sample size of lesions used for LNM due to low number of cases in literature showing images clearly attributable to this population is a further limitation. To account for this and preclude confounding of results due to included thalamic lesions, we have performed leave-one-out cross validation analyses (Supplementary Fig. 3) and repeated LNM calculation masking out the thalamus (Supplementary Fig. 2). Also, the use of a normative connectome from 100 neurotypical young subjects might yield potential instability to our results, although previous LNM studies have reported findings stemming from comparably low connectome subjects.³⁰ Thus, future studies should aim to replicate these results using a larger paediatric

connectome, when available. Furthermore, disease-specific connectomes could better reflect the underlying pathological connectivity state under investigation. However, collecting resting-state fMRI scans from patients with generalized hyperkinetic movement disorders is limited by the need for general anaesthesia or otherwise inevitable movement-related artefacts. Finally, our LNM cohort included patients that were above and below the age range of subjects included in the paediatric connectome. Nonetheless, we aimed to model functional connectivity from lesions acquired during a critical stage of brain development. If more data become available, future studies may use a binned-age version of a connectome that could more accurately match the age-related connectivity model.⁹²

Conclusion

This study provides an overview of lesion distribution in DCP and explores the application of lesion network mapping in this severely disabling condition. The DCP neural network identified here overlaps with previously proposed pathophysiological concepts in hyperkinetic conditions and provides additional insights into potential therapeutic targets. Future work should focus on validating our results in larger prospective cohorts to predict clinical outcome and identify therapeutic targets in DCP.

Supplementary material

Supplementary material is available at *Brain Communications* online.

Funding

The project was funded by the 'Deutsche Forschungsgemeinschaft' (DFG, German Research Foundation), Project-ID 424778381 (Transregional Collaborative Research Centre, CRC TRR 295) to A.A.K. A.L.d.A.M. is a fellow of the Berlin Institute of Health—Charité Clinician Scientist Program and also funded by the DFG, CRC TRR 295 (Project-ID 424778381). A.A.K. is supported by the 'Deutsche Forschungsgemeinschaft' under Germany's Excellence Strategy EXC-2049-390688087 and additionally funded by the Lundbeck Foundation as part of the collaborative project grant "Adaptive and precise targeting of cortex-basal ganglia circuits in Parkinson's Disease" (Grant Nr. R336-2020-1035). A.K. is funded by the University hospital of Cologne. She holds grants from the medical faculty and the Dr. Hans-Günther and Dr. Rita Herfort foundation. M.S.T. is supported by the Edmond J. Safra Fellowship for Movement Disorders of the Michael J. Fox Foundation. The funding sources had no involvement in study design, in the collection, analysis and interpretation of data; in the writing of the manuscript, and in the decision to submit the paper for publication.

Competing interests

A.L.d.A.M., B.A.-F., M.T. and I.-K.M. have no conflicts of interest to declare. A.A.K. has served on advisory boards of Medtronic and has received honoraria and travel support from Medtronic and Boston Scientific outside of this work (both producers of DBS devices). A.K. was PI in the STIM-CP trial, which was partly funded by Boston Scientific.

Data availability

Lesion tracings and lesion network map are available from the corresponding author upon reasonable request. All code used is available within Lead-DBS/-Connectome software (<https://github.com/netstim/leaddbs>).

References

- Rosenbaum P, Paneth N, Leviton A, et al. Proposed definition and classification of cerebral palsy. *Dev Med Child Neurol.* 2007; 47(8):571-571.
- Cans C. Surveillance of cerebral palsy in Europe: A collaboration of cerebral palsy surveys and registers. *Dev Med Child Neurol.* 2000; 42(12):816-824.
- Monbaliu E, de Cock P, Ortibus E, Heyrman L, Klingels K, Feys H. Clinical patterns of dystonia and choreoathetosis in participants with dyskinetic cerebral palsy. *Dev Med Child Neurol.* 2016; 58(2):138-144.
- Bax M, Tydeman C, Flodmark O. Clinical and MRI correlates of cerebral palsy: The European cerebral palsy study. *J Am Med Assoc.* 2006;296(13):1602-1608.
- Sanger TD, Chen D, Fehlings DL, et al. Definition and classification of hyperkinetic movements in childhood. *Mov Disord.* 2010; 25(11):1538-1549.
- Monbaliu E, Himmelmann K, Lin JP, et al. Clinical presentation and management of dyskinetic cerebral palsy. *Lancet Neurol.* 2017; 16(9):741-749.
- Aravamuthan BR, Waugh JL. Localization of basal ganglia and thalamic damage in dyskinetic cerebral palsy. *Pediatr Neurol.* 2016;54:11-21.
- Horber V, Sellier E, Horridge K, et al. The origin of the cerebral palsies: Contribution of population-based neuroimaging data. *Neuropediatrics.* 2020;51(2):113-119.
- Fox MD. Mapping symptoms to brain networks with the human connectome. *N Engl J Med.* 2018;379(23):2237-2245.
- Corp DT, Joutsa J, Ryan Darby R, et al. Network localization of cervical dystonia based on causal brain lesions. *Brain.* 2019;142: 1660-1674.
- Al-Fatly B, Neudorfer C, Kaski D, et al. Lesion network of oculogyric crises maps to brain dopaminergic transcriptomic signature. *Brain.* 2024;147(6):1975-1981.
- Joutsa J, Horn A, Hsu J, Fox MD. Localizing parkinsonism based on focal brain lesions abbreviations: DBS = deep brain stimulation; MSA-P = multiple system atrophy, parkinsonism variant; PSP = progressive supranuclear palsy; STN = subthalamic nucleus. *Brain.* 2018;141(8):2445-2456.
- Laganiere S, Boes AD, Fox MD. Network localization of hemichorea-hemiballismus. *Neurology.* 2016;86(23):2187-2195.
- Ganos C, Al-Fatly B, Fischer JF, et al. A neural network for tics: Insights from causal brain lesions and deep brain stimulation. *Brain.* 2022;145(12):4385-4397.
- Vidailhet M, Yelnik J, Lagrange C, et al. Bilateral pallidal deep brain stimulation for the treatment of patients with dystonia-choreoathetosis cerebral palsy: A prospective pilot study. *Lancet Neurol.* 2009;8(8):709-717.
- Koy A, Kühn AA, Huebl J, et al. Quality of life after deep brain stimulation of pediatric patients with dyskinetic cerebral palsy: A prospective, single-arm, multicenter study with a subsequent randomized double-blind crossover (STIM-CP). *Mov Disord.* 2022;37(4): 799-811.
- Koy A, Kühn AA, Schiller P, et al. Long-term follow-up of pediatric patients with dyskinetic cerebral palsy and deep brain stimulation. *Mov Disord.* 2023;38(9):1736-1742.
- Al-Fatly B, Giesler SJ, Oxenford S, et al. Neuroimaging-based analysis of DBS outcomes in pediatric dystonia: Insights from the GEPESTIM registry. *NeuroImage Clin.* 2023;39:103449.
- Peters M, Godfrey C, McInerney P, Munn Z, Tricco A, Khalil H. JBI manual for evidence synthesis. 2020 Version. (Aromataris E, Munn Z, eds.). 2020.
- Tricco AC, Lillie E, Zarin W, et al. PRISMA extension for scoping reviews (PRISMA-ScR): Checklist and explanation. *Ann Intern Med.* 2018;169(7):467-473.
- Himmelmann K, Horber V, De La Cruz J, et al. MRI classification system (MRICS) for children with cerebral palsy: Development, reliability, and recommendations. *Dev Med Child Neurol.* 2017; 59(1):57-64.
- Amunts K, Lepage C, Borgeat L, et al. BigBrain: An ultrahigh-resolution 3D human brain model. *Science (1979).* 2013; 340(6139):1472-1475.
- Ewert S, Plettig P, Li N, et al. Toward defining deep brain stimulation targets in MNI space: A subcortical atlas based on multimodal MRI, histology and structural connectivity. *Neuroimage.* 2018;170: 271-282.
- Evensen TL, Vik T, Andersen GL, Bjellmo S, Hollung SJ. Prevalence, birth, and clinical characteristics of dyskinetic cerebral palsy compared with spastic cerebral palsy subtypes: A Norwegian register-based study. *Dev Med Child Neurol.* 2023;65(11):1464-1474.
- Kitai Y, Hirai S, Okuyama N, et al. Functional outcomes of children with dyskinetic cerebral palsy depend on etiology and gestational age. *Eur J Paediatr Neurol.* 2021;30:108-112.
- Fonov V, Evans AC, Botteron K, Almli CR, McKinsty RC, Collins DL. Unbiased average age-appropriate atlases for pediatric studies. *Neuroimage.* 2011;54(1):313-327.
- Yushkevich PA, Piven J, Hazlett HC, et al. User-guided 3D active contour segmentation of anatomical structures: Significantly improved efficiency and reliability. *Neuroimage.* 2006;31(3):1116-1128.
- Neudorfer C, Butenko K, Oxenford S, et al. Lead-DBS v3.0: Mapping deep brain stimulation effects to local anatomy and global networks. *Neuroimage.* 2023;268:119862.
- Zuo XN, Anderson JS, Bellec P, et al. An open science resource for establishing reliability and reproducibility in functional connectomics. *Sci Data.* 2014;1(1):1-13.
- Cohen AL, Fox MD. Reply: The influence of sample size and arbitrary statistical thresholds in lesion-network mapping. *Brain.* 2020;143(5):e41-e41.
- Schuch F, Walger L, Schmitz M, et al. An open presurgery MRI dataset of people with epilepsy and focal cortical dysplasia type II. *Sci Data.* 2023;10(1):1-7.
- Himmelmann K, Hagberg G, Wiklund LM, Eek MN, Uvebrant P. Dyskinetic cerebral palsy: A population-based study of children born between 1991 and 1998. *Dev Med Child Neurol.* 2007; 49(4):246-251.
- Krägeloh-Mann I, Helber A, Mader I, et al. Bilateral lesions of thalamus and basal ganglia: Origin and outcome. *Dev Med Child Neurol.* 2002;44(7):477-484.
- Fiori S, Cioni G, Klingels K, et al. Reliability of a novel, semi-quantitative scale for classification of structural brain magnetic resonance imaging in children with cerebral palsy. *Dev Med Child Neurol.* 2014;56(9):839-845.
- Laporta-Hoyos O, Fiori S, Pannek K, et al. Brain lesion scores obtained using a simple semi-quantitative scale from MR imaging

- are associated with motor function, communication and cognition in dyskinetic cerebral palsy. *NeuroImage Clin.* 2018;19:892-900.
36. Romito LM, Zorzi G, Marras CE, Franzini A, Nardocci N, Albanese A. Pallidal stimulation for acquired dystonia due to cerebral palsy: Beyond 5 years. *Eur J Neurol.* 2015;22(3):426-e432.
 37. McClelland VM, Fischer P, Foddai E, et al. EEG measures of sensorimotor processing and their development are abnormal in children with isolated dystonia and dystonic cerebral palsy. *NeuroImage Clin.* 2021;30:102569.
 38. Koy A, Pauls KAM, Flossdorf P, et al. Young adults with dyskinetic cerebral palsy improve subjectively on pallidal stimulation, but not in formal dystonia, gait, speech and swallowing testing. *Eur Neurol.* 2014;72(5-6):340-348.
 39. Van Schie PE, Becher JG, Dallmeijer AJ, Barkhof F, Van Weissenbruch MM, Jeroen Vermeulen R. Motor testing at 1 year improves the prediction of motor and mental outcome at 2 years after perinatal hypoxic-ischaemic encephalopathy. *Dev Med Child Neurol.* 2010;52(1):54-59.
 40. Yilmaz Y, Ekin G. Thalamic involvement in a patient with kernicterus. *Eur Radiol.* 2002;12(7):1837-1839.
 41. Yoshida S, Faria A V, Oishi K, et al. Anatomical characterization of athetotic and spastic cerebral palsy using an atlas-based analysis. *J Magn Reson Imaging.* 2013;38(2):288-298.
 42. Yoshida S, Hayakawa K, Oishi K, et al. Athetotic and spastic cerebral palsy: Anatomic characterization based on diffusion-tensor imaging. *Radiology.* 2011;260(2):511-520.
 43. Okumura A, Hayakawa F, Maruyama K, Kubota T, Kato K, Watanabe K. Single photon emission computed tomography and serial MRI in preterm infants with kernicterus. *Brain Dev.* 2006;28(6):348-352.
 44. Prasad R, Verma N, Srivastava A, Das BK, Mishra OP. Magnetic resonance imaging, risk factors and co-morbidities in children with cerebral palsy. *J Neurol.* 2011;258(3):471-478.
 45. Himmelmann K, Uvebrant P. The panorama of cerebral palsy in Sweden part XII shows that patterns changed in the birth years 2007-2010. *Acta Paediatr.* 2018;107(3):462-468.
 46. Himmelmann K, Hagberg G, Uvebrant P. The changing panorama of cerebral palsy in Sweden. X. Prevalence and origin in the birth-year period 1999-2002. *Acta Paediatrica.* 2010;99(9):1337-1343.
 47. Himmelmann K, Pålman M. The panorama of cerebral palsy in Sweden part XIII shows declining prevalence in birth-years 2011-2014. *Acta Paediatr.* 2023;112(1):124-131.
 48. Saini AG, Sankhyani N, Malhi P, Ahuja C, Khandelwal N, Singhi P. Hyperbilirubinemia and asphyxia in children with dyskinetic cerebral palsy. *Pediatr Neurol.* 2021;120:80-85.
 49. Kitai Y, Hirai S, Okuyama N, et al. Diagnosis of bilirubin encephalopathy in preterm infants with dyskinetic cerebral palsy. *Neonatology.* 2020;117(1):73-79.
 50. Okumura A, Kidokoro H, Shoji H, et al. Kernicterus in preterm infants. *Pediatrics.* 2009;123(6):e1052-e1058.
 51. Kuiper MJ, Meiners LC, Chandler ES, et al. Dyskinesia impairment scale scores in Dutch pre-school children after neonatal therapeutic hypothermia. *Eur J Paediatr Neurol.* 2020;28:70-76.
 52. Gkoltsiou K, Tzoufi M, Counsell S, Rutherford M, Cowan F. Serial brain MRI and ultrasound findings: Relation to gestational age, bilirubin level, neonatal neurologic status and neurodevelopmental outcome in infants at risk of kernicterus. *Early Hum Dev.* 2008;84(12):829-838.
 53. Rutherford MA, Pennock JM, Murdoch-Eaton DM, Cowan FM, Dubowitz LMS. Athetoid cerebral palsy with cysts in the putamen after hypoxic-ischaemic encephalopathy. *Arch Dis Child.* 1992;67(7 Spec No):846-850.
 54. Sugama S, Soeda A, Eto Y. Magnetic resonance imaging in three children with kernicterus. *Pediatr Neurol.* 2001;25(4):328-331.
 55. Kamei A, Sasaki M, Akasaka M, Soga N, Kudo K, Chida S. Proton magnetic resonance spectroscopic images in preterm infants with bilirubin encephalopathy. *J Pediatr.* 2012;160(2):342-344.
 56. Reid SM, Meehan EM, Reddihough DS, Harvey AR. Dyskinetic vs spastic cerebral palsy: A cross-sectional study comparing functional profiles, comorbidities, and brain imaging patterns. *J Child Neurol.* 2018;33(9):593-600.
 57. Sun D, Wang Q, Hou M, et al. Clinical characteristics and functional status of children with different subtypes of dyskinetic cerebral palsy. *Med (United States).* 2018;97(21):e10817.
 58. Laporta-Hoyos O, Pannek K, Ballester-Plané J, et al. White matter integrity in dyskinetic cerebral palsy: Relationship with intelligence quotient and executive function. *NeuroImage Clin.* 2017;15:789-800.
 59. Griffiths PD, Radon MR, Crossman AR, Zurakowski D, Connolly DJ. Anatomic localization of dyskinesia in children with "profound" perinatal hypoxic-ischemic injury. *AJNR Am J Neuroradiol.* 2010;31(3):436-441.
 60. Marks W, Bailey L, Reed M, et al. Pallidal stimulation in children: Comparison between cerebral palsy and DYT1 dystonia. *J Child Neurol.* 2013;28(7):840-848.
 61. Derinkuyu BE, Ozmen E, Akmaz-Unlu H, Altinbas NK, Gurkas E, Boyunaga O. A magnetic resonance imaging finding in children with cerebral palsy: Symmetrical central tegmental tract hyperintensity. *Brain Dev.* 2017;39(3):211-217.
 62. Cajigas I, Morrison MA, Luciano MS, Starr PA. Cerebellar deep brain stimulation for the treatment of movement disorders in cerebral palsy. *J Neurosurg.* 2023;139(3):605-614.
 63. Qin Y, Li Y, Sun B, et al. Functional connectivity alterations in children with spastic and dyskinetic cerebral palsy. *Neural Plast.* 2018;(Article ID 7058953):7058953.
 64. Qin Y, Sun B, Zhang H, et al. Aberrant interhemispheric functional organization in children with dyskinetic cerebral palsy. *Biomed Res Int.* 2019;2019(1):4362539.
 65. Park BH, Park SH, Seo JH, Ko MH, Chung GH. Neuroradiological and neurophysiological characteristics of patients with dyskinetic cerebral palsy. *Ann Rehabil Med.* 2014;38(2):189-199.
 66. Ballester-Plané J, Schmidt R, Laporta-Hoyos O, et al. Whole-brain structural connectivity in dyskinetic cerebral palsy and its association with motor and cognitive function. *Hum Brain Mapp.* 2017;38(9):4594-4612.
 67. Prél M, Rackauskaite G, Larsen ML, et al. Children with dyskinetic cerebral palsy are severely affected as compared to bilateral spastic cerebral palsy. *Acta Paediatr.* 2019;108(10):1850-1856.
 68. Luciano MS, Robichaux-Vichoever A, Dodenhoff KA, et al. Thalamic deep brain stimulation for acquired dystonia in children and young adults: A phase 1 clinical trial. *J Neurosurg Pediatr.* 2020;27(2):203-212.
 69. Towsley K, Shevell MI, Dagenais L. Population-based study of neuroimaging findings in children with cerebral palsy. *Eur J Paediatr Neurol.* 2011;15(1):29-35.
 70. Himmelmann K, Uvebrant P. Function and neuroimaging in cerebral palsy: A population-based study. *Dev Med Child Neurol.* 2011;53(6):516-521.
 71. Krägeloh-Mann I. Imaging of early brain injury and cortical plasticity. *Exp Neurol.* 2004;190(Suppl. 1):84-90.
 72. Johnston M V, Trescher WH, Ishida A, Nakajima W. The developing nervous system: A series of review articles: Neurobiology of hypoxic-ischemic injury in the developing brain. *Pediatr Res.* 2001;49:735-741.
 73. Tambasco N, Romoli M, Calabresi P. Selective basal ganglia vulnerability to energy deprivation: Experimental and clinical evidences. *Prog Neurobiol.* 2018;169:55-75.
 74. Watchko JF, Tiribelli C. Bilirubin-induced neurologic damage — Mechanisms and management approaches. *N Engl J Med.* 2013;369(21):2021-2030.
 75. Miller SP, Ramaswamy V, Michelson D, et al. Patterns of brain injury in term neonatal encephalopathy. *J Pediatr.* 2005;146(4):453-460.
 76. Myers RE. Two patterns of perinatal brain damage and their conditions of occurrence. *Am J Obstet Gynecol.* 1972;112(2):246-276.

77. Foster NN, Barry J, Korobkova L, et al. The mouse cortico–basal ganglia–thalamic network. *Nordisk Alkohol Nark.* 2021; 598(7879):188-194.
78. Mohammad SS, Angiti RR, Biggin A, et al. Magnetic resonance imaging pattern recognition in childhood bilateral basal ganglia disorders. *Brain Commun.* 2020;2(2):fcaa178.
79. Pearson TS, Pons R, Ghaoui R, Sue CM. Genetic mimics of cerebral palsy. *Mov Disord.* 2019;34(5):625-636.
80. Solé-Padullés C, Castro-Fornieles J, De La Serna E, et al. Intrinsic connectivity networks from childhood to late adolescence: Effects of age and sex. *Dev Cogn Neurosci.* 2016;17:35-44.
81. Sussman BL, Wyckoff SN, Heim J, et al. Is resting state functional MRI effective connectivity in movement disorders helpful? A focused review across lifespan and disease. *Front Neurol.* 2022;13: 847834.
82. Tsagkaris S, Yau EKC, McClelland V, et al. Metabolic patterns in brain 18F-fluorodeoxyglucose PET relate to aetiology in paediatric dystonia. *Brain.* 2023;146(6):2512-2523.
83. Kerrigan JF, Chugani HT, Phelps ME. Regional cerebral glucose metabolism in clinical subtypes of cerebral palsy. *Pediatr Neurol.* 1991;7(6):415-425.
84. Kim JS. Delayed onset mixed involuntary movements after thalamic stroke: Clinical, radiological and pathophysiological findings. *Brain.* 2001;124(2):299-309.
85. Shine JM, Lewis LD, Garrett DD, Hwang K. The impact of the human thalamus on brain-wide information processing. *Nat Rev Neurosci.* 2023;24(7):416-430.
86. Gaidica M, Hurst A, Cyr C, Leventhal DK. Distinct populations of motor thalamic neurons encode action initiation, action selection, and movement vigor. *J Neurosci.* 2018;38(29):6563-6573.
87. Sauerbrei BA, Guo JZ, Cohen JD, et al. Cortical pattern generation during dexterous movement is input-driven. *Nordisk Alkohol Nark.* 2019;577(7790):386-391.
88. Koy A, Hellmich M, Pauls KAM, et al. Effects of deep brain stimulation in dyskinetic cerebral palsy: A meta-analysis. *Mov Disord.* 2013;28(5):647-654.
89. Young SJ, Bertuccio M, Sanger TD. Cathodal transcranial direct current stimulation in children with dystonia: A sham-controlled study. *J Child Neurol.* 2014;29(2):232-239.
90. Ueda K, Aravamuthan BR, Pearson TS. Dystonia in individuals with spastic cerebral palsy and isolated periventricular leukomalacia. *Dev Med Child Neurol.* 2023;65(1):94-99.
91. Boes AD, Prasad S, Liu H, et al. Network localization of neurological symptoms from focal brain lesions. *Brain.* 2015;138(10):3061-3075.
92. Bdaiwi AS, Greiner HM, Leach J, Mangano FT, DiFrancesco MW. Categorizing cortical dysplasia lesions for surgical outcome using network functional connectivity. *J Neurosurg Pediatr.* 2021;28(5): 600-608.